Original Article

ENERGY EXPLORATION & EXPLOITATION

Energy Exploration & Exploitation
2016, Vol. 34(5) 735–745

DOI: 10.1177/0144598716656067
eea.sagepub.com
SAGE

Binding characteristics of Cd^{2+}, Zn^{2+}, Cu^{2+}, and Li^{+} with humic substances: Implication to trace element enrichment in low-rank coals

Hong-Tao He,[1,2] Le-Cai Xing,[1,2] Jing-Sen Zhang[1,2] and Mao Tang[3]

Abstract

Binding characteristics of metal ions (Li^{+}, Cd^{2+}, Zn^{2+}, Cu^{2+}) with humic substances (HSs) are investigated by first principle calculation at BP86/SDD level. In the present work, HSs are well represented by singly deprotonated alkyl/aryl carboxylic acid. The results reveal that the bidentate is the strongest complexation form. Moreover, with the increase of ionic potential, the binding energies of HSs to chelate metal ions increase in order, $Li^{+} < Cd^{2+} < Zn^{2+} < Cu^{2+}$. The nature of the ligand also exerts important influence on the stability of organometallic complexes. Specifically, for Li^{+}, the ionic bond-forming part occurs as electroneutrality. Whatever electron-donating groups or electron-withdrawing groups including alkyl, aryl and its derivatives (salicylic acid and m (p)-substituted gallic acid by hydroxyl or amino) and carbon-carbon double bond connects to the carboxylate group, the electron density of the ionic bond-forming part will be changed resulting in the decrease of binding energy (BE). However, for ions with high ionic potential or high positive charge density (Cd^{2+}, Cu^{2+} and Zn^{2+}), the ionic bond-forming part is positively charged. From electron-withdrawing groups to electron-donating groups, the extent to deviate from electroneutrality is gradually decreased, although the quantity of electron is possibly insufficient to balance the extra positive charge. As a result, the BE value gradually increases, but does not reach a maximum for studied ions and ligands. Besides, mixed functional groups are able to stabilize organometallic complexes. The optimal mixed functional group is carboxyl and hydroxyl on ortho position, followed by two hydroxyls, hydroxyl and carbonyl, carboxyl and carbonyl,

[1]Key Laboratory of Resource Survey and Research of Hebei Province, Hebei University of Engineering, Handan, Hebei, China
[2]Collaborative Innovation Center of Coal Exploitation, Hebei University of Engineering, Handan, Hebei, China
[3]State Key Laboratory of Ore Deposit Geochemistry, Institute of Geochemistry, Chinese Academy of Sciences, Guiyang, China

Corresponding author:
Mao Tang, State Key Laboratory of Ore Deposit Geochemistry, Institute of Geochemistry, Chinese Academy of Sciences, Guiyang 550081, China.
Email: tangmao@vip.gyig.ac.cn

two carboxyls. Strong electron-withdrawing effect attributes to the decrease of the BE value for the latter three.

In the end, the geochemical behavior of trace elements in coalification is predicted: small organic acids generated by decomposition of dead plants in relatively oxidized environments will facilitate the enrichment of lithium and this proportion of lithium will be released into pore water in the polymerization of small molecules, possibly accumulating in secondary minerals in low-rank coals; metal ions with high ionic potential bonded by organic molecules will be released in a later stage and accumulate in slightly higher rank coals.

Keywords
Low-rank coal, element enrichment, binding energy, first principle calculation

Introduction

Recently, a variety of trace elements including Li, Ge, U, Hg is reported to be enriched in coal seams worldwide (Dai et al., 2014; Qin et al., 2015a, 2015b; Seredin et al., 2013; Sun, 2015; Sun et al., 2012, 2013a, 2013b, 2016). Most of these studies focused on the anomalous concentration of trace elements in coals and the affinity of these elements to the organic matters or the inorganic parts can be discerned on the level of mineral (Chu et al., 2015; Kang et al., 2014). However, the studies on the enrichment mechanisms and the origin of these elements in coals are scared (Qin et al., 2015b) and badly needed. Ambiguous recognition to these key problems brings about the low efficiency of coal utilization and extreme exacerbation of the environment due to the release of hazardous elements. To probe the modes of occurrence of trace elements in details, i.e. the chemical bonding environments around the trace element atom of interest will shed light on the enrichment mechanism and provide suggestions to coal clean utilization.

To deduce the enrichment process is a difficult work since the coalification is sluggish and the structure of coal is complex. From this perspective, except vibrational spectroscopy, ab initio or first principle calculation is the best selection to assist unraveling this scenario. First principle calculations are supposed to provide exact electronic structure calculation and molecular dynamic simulation.

Besides the way to be brought by hydrothermal fluids, valuable/hazardous elements can also be enriched in peat or low-rank coals at (syn-) sedimentary stage (Sun et al., 2010; Wang et al., 2015). The structure of the peat or the low-rank coal can be represented by humic substances (HSs). This facilitates the simulation of element enrichment in coals since candidates of HSs structure are intensively researched in previous studies (Gao et al., 2015; Ramalho et al., 2007; Sviatenko et al., 2016; Zhu et al., 2015). Although the concrete molecular structure of HSs has yet not been determined due to its large molecular size and complexity, the main functional groups able to form complex with metals include carboxyl, hydroxyl, and phenol of local configuration. Sundararajan et al. (2011) showed that the predominant of adsorptive site for uranyl ion was the carboxyl and the functional groups nearby might aid the chelation. For other metal ions with smaller size, whether identical adsorption behaviors can be observed has yet not been intensively investigated. In the present study, first principle calculations are employed to investigate the characteristics of Li^+, Cu^{2+}, Cd^{2+}, and Zn^{2+} bonded to

Table 1. The symmetric ν_s(C=O) strength mode calculated at different levels.

Method	*Symmetric ν_s(C=O) strength mode*
BP86/SDD	1710.54 cm^{-1}
BP86/TZVP	1793.26 cm^{-1}
BP86/def2-SVP	1838.42 cm^{-1}
BP86/def2-QZVP	1787.84 cm^{-1}
BP86/6-31G(d)	1827.20 cm^{-1}
B3LYP/6-31G(d)	1892.06 cm^{-1}
B3LYP/6-311G(d)	1877.38 cm^{-1}
Experimental data	1710.40 cm^{-1}

Experimental data comes from Ibrahim (2009).

HSs, mimicking the enrichment of element in coals. Specifically, we focus on the ability of all favorable functional groups to chelate metal ions in terms of binding energy (BE) and discuss the factors influencing the stability of complexes.

Calculation methods

First principle calculations are employed to probe the ability of HSs to enrich metal ions. Seven methods are tested to choose the proper method, shown in Table 1. Table 1 shows comparison of calculated characteristic ν_s(C=O) with experimental data. In this study, tests are carried out on single CH_3COOH molecule.

From Table 1, the symmetric ν_s(C=O) strength mode calculated at BP86/SDD level is in good agreement with the experimental data. At the same time, we have compared the optimized geometry ($Cd(H_2O)_6^{2+}$ at BP86/SDD level) with EXAFS data (2.27 Å vs. 2.30 Å, Vasconcelos et al., 2008). In the end, this level has been selected to optimize geometry and calculate BE since its good performance and rather lower computational cost (not shown).

Geometry optimizations are carried out for all candidates of HSs, including multiple adsorption sites on one candidate (Figure 1). Additionally, harmonic vibrational frequencies were analyzed to ensure that the geometries obtained represent local minima, to say the least, on the potential surface. All calculations are implemented with the GAUSSIAN09 software package (Frisc et al., 2010). Computational resources for the present work are provided by the National Supercomputer Center in Guangzhou (NSCC-GZ).

Herein, the binding energies of functional groups to chelate Cd^{2+}, Zn^{2+}, Cu^{2+}, and Li^{+} are calculated with BP86/SDD level, in which all atoms are described by Stuttgart/Dresden ECP. The specific calculation of BE follows:

$$BE = E_{\text{complex}} - E_{\text{cation}} - E_{\text{ligand}} + \Delta\text{ZPVE} \quad (1)$$

where E_{complex}, E_{cation}, and E_{ligand} represent the electronic energy of complex, cations, and ligands, respectively, while ΔZPVE for the calibration of zero point vibrational energy.

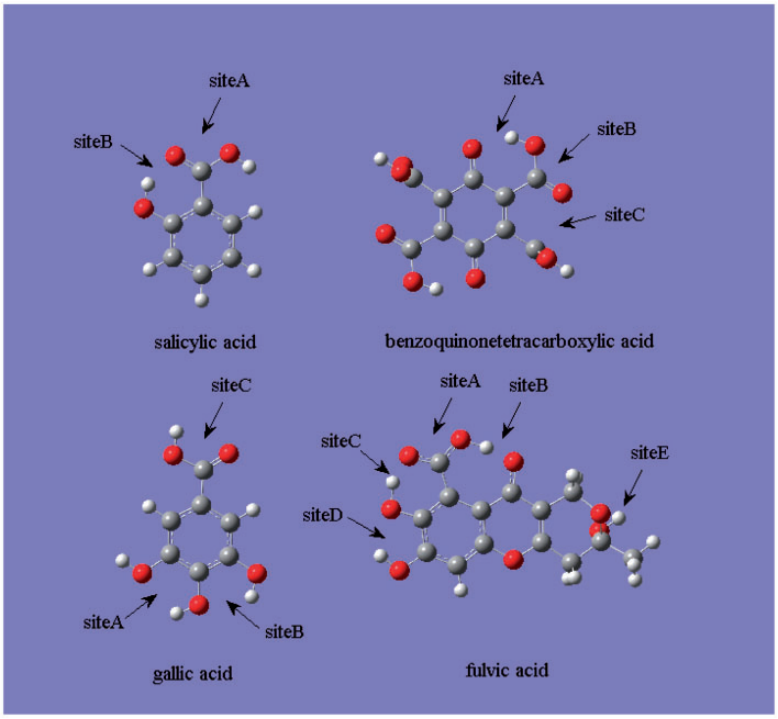

Figure 1. Multiple adsorption sites on HSs candidates involved.

Results and discussion

Geometry of adsorbed metal ions

The most stable metal-ligand complexes occur as bidentates shown in Figure 2 (similar geometries of Cd^{2+}, Zn^{2+} and Cu^{2+} are not shown herein). It can be seen that except the carboxylate anion, ortho-substituted oxygen-containing groups on benzene or heterocyclic organics are either able to stably chelate metal ions. Specifically, in the case of carboxylate, both the oxygen atom from deprotonated hydroxyl and the oxygen from carbonyl all take part in binding with Li^{+}. Whilst in other cases, part of carboxyl participates chelation together with neighbor functional groups including hydroxyl, the other carboxyl or quinone groups. Besides, two hydroxyl groups can also complete the chelation.

The role of ionic potential of cations

As is shown in Figure 3 and Table 2, with the increase of ionic potential, the binding energies of all functional groups with metals increase from ca. 600 kJ/mol to 2000 kJ/mol, showing the identical trend for four metal ions. Although Cd^{2+}, Zn^{2+}, and Cu^{2+} are separated into borderline ion category, which seek for nitrogen/sulfur in organic matters, while Li^{+} referred as hard ion category seeking for oxygen, they can form more stable complexes when reacting with oxygen-containing functional groups relative to hard ions (Nieboer and Richardson, 1980). This statement greatly agrees with our results.

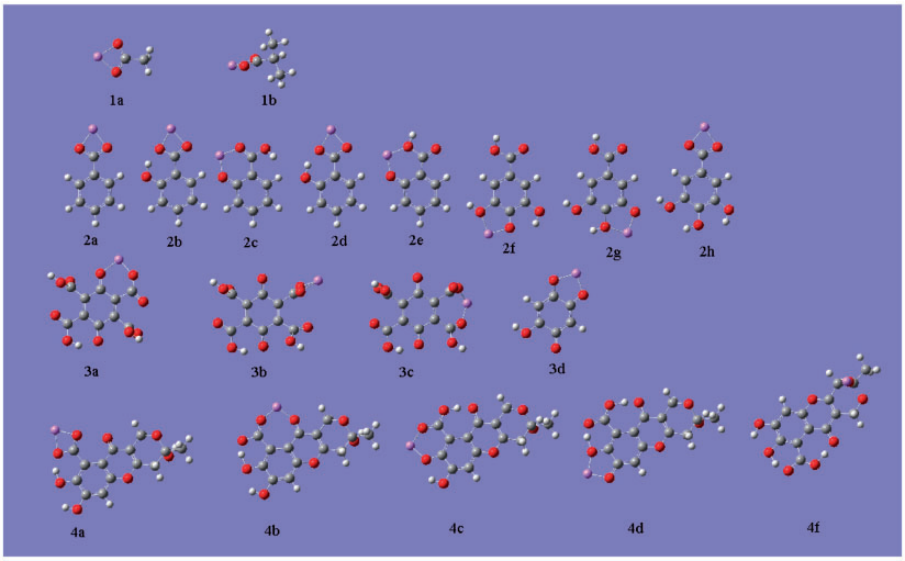

Figure 2. The binding types of ions to different candidates of HSs.
In specific, the atom in purple is Li, while grey is C, red is O, and white is H. The ligand in 1a is deprotonated acetic acid, while 1b deprotonated 2-methyl-propionic acid, 2a deprotonated benzoic acid, 2b-e deprotonated salicylic acid, 2f-h deprotonated gallic acid, 3a-c deprotonated benzoquinonetetracarboxylic acid, 3d deprotonated 2,5-dihydroxy-benzoquinone, 4a-e deprotonated fulvic acid (rebuilt from Sundararajan et al., 2011).

The role of ligand

The nature of the ligand, specific functional group, and the combination of multiple functional groups on local configurations of HSs determine the ability of ligand to chelate metal ions.

The binding energies for the single functional group of the ligands to chelate metal ions are depicted in Figure 4. In general, the carboxyl is considered as the main adsorption site. From Figure 3 and Figure 4, one can learn that due to the limitation of electron transferring/sharing, hydrated metal ions almost have the lowest BE values. Admittedly, the negative charge generated by the deprotonation of carboxyl needs to be delocated, i.e. sharing by carbon and oxygen in the conjugated system, which is necessary for the stabilization of carboxylate anion. We speculate the more charge remains on carboxylate anion whatever positive or negative, the less stable the complex is. In the case of Li^+, the ionic bond-forming part occurs as electroneutrality. When strong electron-withdrawing group like carbon–carbon double bond connects to the carboxylate, the electron will be strongly withdrawn from the carboxylate anion resulting in the deviation from electroneutrality for the ionic bond-forming part. This largely reduces the stability of complex. Due to the fact that ortho hydroxyl forms hydrogen bond with benzoic acid and develops steric hindrance, the destruction of conjugation between the aryl and the carboxylate changes benzene ring of the salicylic acid from week electron-donating group to electron-withdrawing group. It also deviates

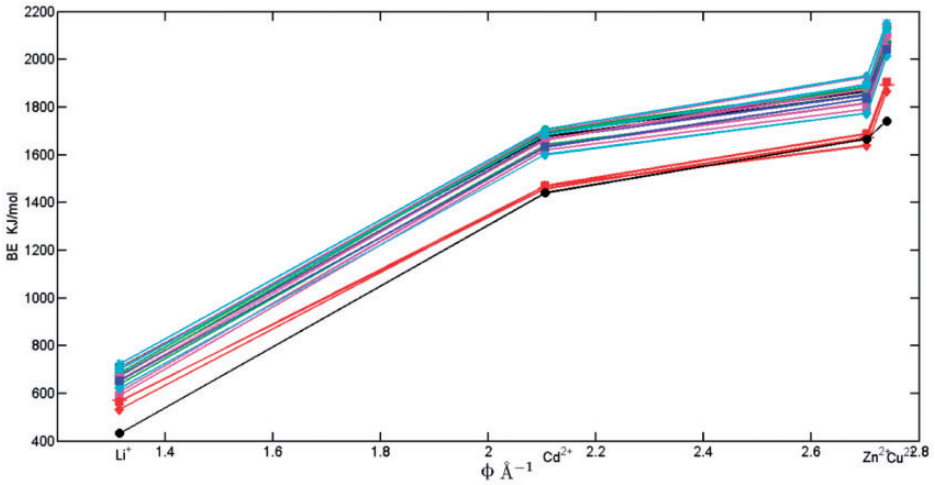

Figure 3. The binding energy of complexes variation with the ionic potential of cations. BE stands for binding energy. Notations: Φ is the calculated ionic potential for Li^{+}(1.32Å^{-1}), Cd^{2+}(2.11Å^{-1}), Zn^{2+}(2.70Å^{-1}), and Cu^{2+}(2.74Å^{-1}), based on the ionic radii of Shannon (1976). The binding energy curves are specified as black square (deprotonated acetic acid), black star (deprotonated 2-methyl-propionic acid), and blue diamond (deprotonated benzoic acid), green diamond (deprotonated gallic acid siteA), green circle (deprotonated gallic acid siteB), green square (deprotonated gallic acid siteC), carmine square (deprotonated fulvic acid siteA), carmine circle (deprotonated fulvic acid siteB), carmine diamond (deprotonated fulvic acid siteC), carmine star (deprotonated fulvic acid siteD), carmine plus (deprotonated fulvic acid siteE), cyan plus (deprotonated salicylic_acid_siteA_1), cyan star (deprotonated salicylic_acid_siteB_1), cyan diamond (deprotonated salicylic_acid_siteA_3), cyan square (deprotonated salicylic_acid_siteB_3), blue square (deprotonated 2,5-dihydroxy-benzoquinone), red square (deprotonated benzoquinonetetracarboxylic acid siteA), red diamond (deprotonated benzoquinonetetracarboxylic acid siteB), red plus (deprotonated benzoquinonetetracarboxylic acid siteC), and black circle (H_2O). Please refer to Table 2 in detail.

the electroneutrality, then decreases the BE value of organolithium complex, although the extent is lower than that corresponding to deprotonated benzoquinonetetracarboxylic acid. Moreover, when Li^{+} is chelated by functional groups being less influenced by apparent electronic effect (electron-donating effect or electron-withdrawing effect) like alcohol and formic acid, the BE value increases for the further less deviation from electroneutrality. When methyl or isopropyl connects to the carboxylate, the ionic bond-forming part gains more electrons since the alkyl is electron-donating group. The more the methyl directly/indirectly connects to the central carbon of the carboxylate, the more electrons are obtained. This arrangement will convert the ionic bond-forming part from electroneutrality to electronegativity decreasing the stability of organolithium complex. Comparing to the alkyl, the aryl and its derivatives (m (p)-substituted gallic acid by hydroxyl or amino) conjugated with the carboxylate can offer even more electrons since electrons belonging to big π and p-π conjugated systems can be delocated into the carboxylate and elevate its electron density. It is clear that for organolithium complexes, deviations from electroneutrality on ionic

Table 2. Binding energies of all complexes.

Ligands	$E_{ligands}$ (hartree)	$E_{Cd\text{-}complexes}$ (hartree)	$E_{Zn\text{-}complexes}$ (hartree)	$E_{Li\text{-}complexes}$ (hartree)	$E_{Cu\text{-}complexes}$ (hartree)	$BE_{Cd\text{-}complexes}$ (kJ/mol)	$BE_{Zn\text{-}complexes}$ (kJ/mol)	$BE_{Li\text{-}complexes}$ (kJ/mol)	$BE_{Cu\text{-}complexes}$ (kJ/mol)
CH_3COO^-	−228.454	−395.962	−455.357	−235.999	−425.569	−1677.0	−1853.1	−710.1	−2063.5
$CH_3CHCOOCH_3^-$	−307.014	−474.527	−533.922	−314.556	−504.132	−1690.9	−1865.7	−700.3	−2071.8
$C_6H_5COO^-$	−420.128	−587.633	−647.031	−427.661	−617.246	−1666.8	−1850.7	−676.3	−2071.7
$C_6H_3O_4^-$	−531.260	−698.752	−758.157	−538.784	−728.367	−1632.4	−1835.2	−652.6	−2042.2
gallic_acid_siteA	−645.800	−813.295	−872.689	−653.319	−842.921	−1641.6	−1815.3	−640.1	−2079.9
gallic_acid_siteB	−645.775	−813.293	−872.689	−653.311	−842.917	−1702.0	−1881.6	−686.1	−2135.2
gallic_acid_siteC	−645.782	−813.297	−872.693	−653.312	−842.916	−1694.9	−1873.9	−669.5	−2114.1
salicylic_acid_siteA_1	−495.384	−662.863	−722.257	−502.896	−692.480	−1601.3	−1774.7	−621.5	−2014.2
salicylic_acid_siteB_1	−495.339	−662.859	−722.271	−502.890	−692.488	−1707.3	−1929.9	−724.5	−2153.2
salicylic_acid_siteA_3	−495.384	−662.863	−722.257	−502.896	−692.480	−1601.4	−1774.7	−621.5	−2014.2
salicylic_acid_siteB_3	−495.345	−662.856	−722.263	−502.887	−692.484	−1685.1	−1892.4	−700.6	−2126.9
fulvic_acid_SiteA	−1141.688	−1309.174	−1368.568	−1149.189	−1338.795	−1619.8	−1791.5	−592.4	−2042.9
fulvic_acid_SiteB	−1141.688	−1309.190	−1368.607	−1149.219	−1338.819	−1660.2	−1894.7	−672.3	−2104.6
fulvic_acid_SiteC	−1141.682	−1309.198	−1368.613	−1149.225	−1338.828	−1698.6	−1927.3	−703.1	−2146.4
fulvic_acid_SiteD	−1141.704	−1309.208	−1368.616	−1149.229	−1338.830	−1665.5	−1874.2	−655.1	−2091.6
fulvic_acid_SiteE	−1141.684	−1309.177	−1368.574	−1149.190	−1338.798	−1636.0	−1816.6	−605.3	−2059.3
$C_{10}O_{10}H_3$_siteA_3	−1135.001	−1302.431	−1361.842	−1142.492	−1332.056	−1470.2	−1687.6	−565.2	−1904.8
$C_{10}O_{10}H_3$_siteB_3	−1135.001	−1302.431	−1361.823	−1142.480	−1332.042	−1469.8	−1638.9	−533.0	−1867.7
$C_{10}O_{10}H_3$_siteC_3	−1135.001	−1302.426	−1361.835	−1142.494	−1332.052	−1458.0	−1670.2	−570.0	−1893.9
H_2O	−76.395	−625.788	−685.202	−236.625	−655.362	−1440.7	−1661.1	−432.3	−1741.9
$HCOO^-$	−189.166	–	–	−196.708	–	–	–	−701.0	–
NH_2_4_gallic_acid_siteC	−625.900	–	–	–	−823.064	–	–	–	−2192.7
CH_3O_4_gallic_acid_siteC	−685.042	–	–	–	−882.182	–	–	–	−2130.6
NH_2_3,4,5_gallic_acid_siteC	−586.132	−753.694	−813.090	–	−783.317	−1819.2	−1996.9	–	−2248.0

The energies in unit of hartree of Cd^{2+}, Zn^{2+}, Cu^{2+} and Li^+ are −166.870, −226.198, −196.329, and −7.275, respectively.
NH_2_4_gallic_acid_siteC (deprotonated 4-aminogallic acid), CH_3O_4_gallic_acid_siteC (deprotonated 4-Methoxygallic acid), NH_2_3,4,5_gallic_acid_siteC (deprotonated 3,4,5-TRIAMINOGALLIC acid), other ligands in Figure 2.

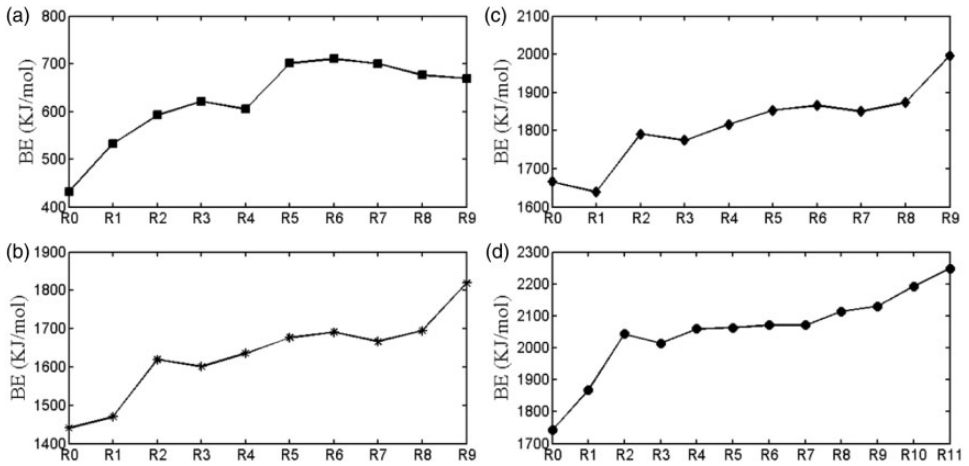

Figure 4. The binding energies corresponding to a single functional group on the ligand to chelate Li^+ (a), Cd^{2+} (b), Zn^{2+} (c), and Cu^{2+}(d).

The expression of adsorbed metal ion is referred as RMe (Me stands for metal ions, while R is the single functional group involved in chelation. Notation: in subplot a, R0 (H_2O), R1–R9 (carboxylate/hydroxo-containing HSs, specifically, benzoquinonetetracarboxylic acid, fulvic acid (refer to carboxylate), salicyclic acid, fulvic acid (refer to hydroxo group), formic acid, acetic acid, 2-methyl-propionic acid, benzoic acid, gallic acid, following the increase of positive charge remained in ionic bond-forming part. In subplots b and c, R0 (H_2O), R1–R9 (carboxylate/hydroxo-containing HSs, specifically, benzoquinonetetracarboxylic acid, fulvic acid (refer to carboxylate), salicyclic acid, fulvic acid (refer to hydroxo group), acetic acid, 2-methyl-propionic acid, benzoic acid, gallic acid, 3,4,5-Triaminogallic acid. In subplot d, R0 (H_2O), R1–R11 (carboxylate/hydroxo-containing HSs, specifically, benzoquinonetetracarboxylic acid, fulvic acid (refer to carboxylate), salicyclic acid, fulvic acid (refer to hydroxo group), acetic acid, 2-methyl-propionic acid, benzoic acid, gallic acid, 4-methoxygallic acid, 4-aminogallic acid, and 3,4,5-triaminogallic acid.

bond-forming part all decrease the BE values (Figure 4). Therefore, the maximum of BE value occurs at the vicinity of lithium acetate.

However, for borderline ions, due to the high ionic potential or positive charge density, the ionic bond-forming part is positively charged. From benzoquinonetetracarboxylic acid to 3,4,5-triaminogallic acid, the quantity of electron obtained by the carboxylate anion gradually increases, with the synchronous decrease of the extent to deviate from electroneutrality. This process will increase the BE value. That the BE values for Cd^{2+}, Zn^{2+} and Cu^{2+} do not reach the maxima in our study possibly attributes to the insufficient electron gained by the carboxylate to balance the positive charge. It is not unconceivable that the BE value hardly reaches the maximum especially for high strength field element like REE^{3+}. From the perspective of element enrichment and heavy metal removal, the quantity of low-rank coal seems to be the sole factor considered for ions with high ionic potential.

The strongest combination of mixed functional groups to chelate metal ions is hydroxyl and carboxyl (supported by Sundararajan et al., 2011), followed by two hydroxyls, hydroxyl and carbonyl, carboxyl and carbonyl, two carboxyls in the decreasing order (Figure 5). As to this sequence, the latter three are largely influenced by electron-withdrawing groups, i.e. carbon–carbon double bond or carbon–oxygen double bond in the candidates selected.

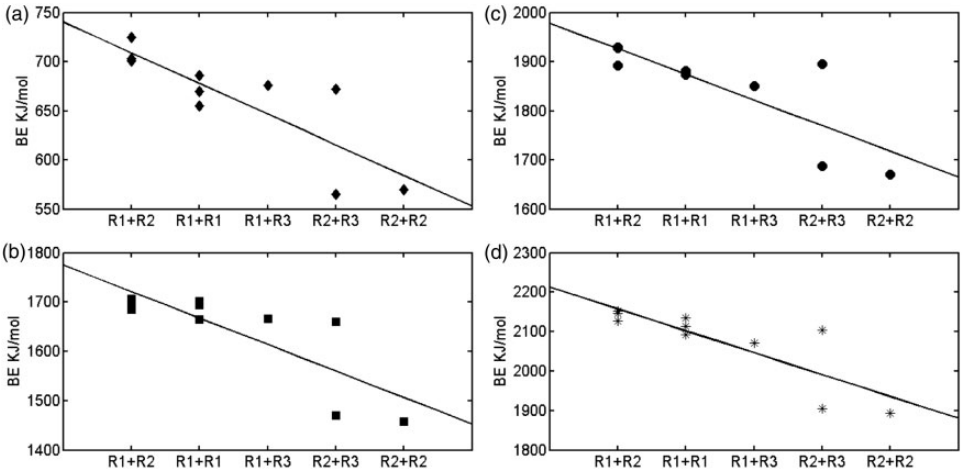

Figure 5. The binding energies of mixed functional groups to chelate metals, Li^{+}(a), Cd^{2+}(b), Zn^{2+}(c), and Cu^{2+}(d). BE, binding energy; R1, hydroxyl; R2, carboxyl; R3, carbonyl.

On the other hand, the decrease of BE values seemly correlates with the combinations, albeit the absence of a proper quantity needed to describe the x dimension. In future, more detailed works are needed to probe the ability of mixed functional groups in distinct chemical environments to chelate metal ions.

Implication to the enrichment of elements in coals

In our calculations, HSs show considerable potential to chelate metal ions, which maybe an important process to accumulate valuable/hazardous element in peats. Coincident with gradual coalification, simple organic molecules condense into large molecule and oxygen-containing functional groups on side chains are cut in further compaction and metamorphism. In this process, the number of hydroxyl and carboxyl rapidly diminishes and carboxyl is nearly lost in typical bituminous coals. The diminishment of these main functional groups able to chelate metal ions exerts an important influence on the variation of trace element in the organic fraction, which maybe assist the conversion between organic affinity and inorganic affinity.

In relatively oxidized environments, the dead plants are decomposed into small organic acid which facilitates the enrichment of lithium. When small molecules are polymerized, Li^{+} delivered by small molecules will be released into pore water with a considerable amount. This proportion of ions may enter into the epigenic minerals with low solubility or the leaching fluids off the coal seams. Lithium is expected to be enriched in low-rank coals. However, for metal ions with high ionic potential like Cd^{2+}, Cu^{2+}, Zn^{2+}, even REE^{3+}, these elements will be largely enriched in weekly oxidized environments where relatively large organic molecules containing conjugated electron-donating groups like benzene ring and its derivatives are predominant. These elements will be possibly accumulated in slightly higher rank coals.

In fact, high concentrations of trace element in coals are supposed to be ascribed to elevated content of secondary minerals therein, which is obvious for the vitrinite and the inertinite (Sun et al., 2013a). Trace element bounded to the organic fraction only contributes to a little proportion of the total amount. Based on our calculations, HSs or macerals indeed

serve as a transporter. Chelation by simple organic acids and re-release during the formation of macromolecules promote to the transportation and subsequent local accumulation of trace elements, for example in plant cells. However, details involved have yet not been unambiguously understood. Eventually, the geochemical behaviors of trace elements in coalification are complex. More researches are needed to resolve these puzzles.

Conclusions

In the present study, we optimized organometallic complex geometries and calculate binding energies of HSs to chelate metal ions (Li^+, Cd^{2+}, Zn^{2+}, Cu^{2+}). Main findings are listed here:

(1) The most stable organometallic complexes are bidentates.
(2) With the increase of ionic potential, the binding energies of HSs to chelate metal ions increase in order, $Li^+ < Cd^{2+} < Zn^{2+} < Cu^{2+}$.
(3) In response to the decrease of the extent to deviate from electroneutrality for the ionic bond-forming part, an obvious increase of BE is found for Cd^{2+}, Cu^{2+} and Zn^{2+} and the maximum does not appear in our study. In the case of Li^+, the maximum of BE occurs at the vicinity of lithium acetate.
(4) The intensity of influence from mixed functional groups on the stability of complex follows the order: carboxyl + hydroxyl > two hydroxyls > hydroxyl + carbonyl > carboxyl + carbonyl > two carboxyls. Strong electron-withdrawing effect attributes to the decrease of the BE value for the latter three.
(5) We predict the geochemical behavior of trace elements in coalification: small organic acids generated by decomposition of dead plants in relatively oxidized environments will facilitate the enrichment of lithium and this proportion of lithium will be released into pore water in the polymerization of small molecules, possibly accumulating in secondary minerals in low-rank coals; metal ions with high ionic potential bonded by organic molecules will be released in a later stage and accumulate in slightly higher rank coals.

Acknowledgment

The author thank Dr Zhao Cunliang for detailed discussion.

Declaration of conflicting interests

The author(s) declared no potential conflicts of interest with respect to the research, authorship, and/or publication of this article.

Funding

The author(s) disclosed receipt of the following financial support for the research, authorship, and/or publication of this article: State Natural Sciences Foundation Monumental Projects (No. 41490635) and key program (No. 41330317).

References

Chu GC, Xiao L, Jin Z, et al. (2015) The relationship between trace element concentrations and coal-forming environments in the No.6 coal seam, Haerwusu Mine, China. *Energy Exploration & Exploitation* 33(1): 91–104.

Dai S, Liu J, Vladimir V, et al. (2014) Composition and modes of occurrence of minerals and elements in coal combustion products derived from high-Ge coals. *International Journal of Coal Geology* 121: 79–97.

Frisc MJ, Trucks GW, Schlegel HB, et al. (2010) *Gaussian 09 (Revision C.01)*. Wallingford: Gaussian, Inc.

Gao X, Yang G, Tian R, et al. (2015) Formation of sandwich structure through ion adsorption at the mineral and humic interfaces: A combined experimental computational study. *Journal of Molecular Structure* 1093: 96–100.

Ibrahim M (2009) Molecular modeling and FTIR study for K, Na, Ca and Mg coordination with organic acid. *Journal of Computational and Theoretical Nanoscience* 6(3): 682–685.

Kang J, Zhao L, Wang XB, et al. (2014) Abundance and geological implication of rare earth elements and yttrium in coals from the Suhaitu Mine, Wuda Coalfield, northern China. *Energy Exploration and Exploitation* 32(5): 873–890.

Nieboer E and Richardson DHS (1980) The replacement of the nondescript term 'heavy metals' by a biologically and chemically significant classification of metal ions. *Environmental Pollution (series B)* 1: 3–26.

Qin SJ, Sun YZ, Li YH, et al. (2015a) Coal deposits as promising alternative sources for gallium. *Earth-Science Reviews* 150: 95–101.

Qin SJ, Zhao CL, Li YH, et al. (2015b) Review of coal as a promising source of lithium. *International Journal of Oil, Gas and Coal Technology* 9(2): 215–229.

Ramalho TC, Cunda EFF, Alencastro RB, et al. (2007) Differential complexation between Zn^{2+} and Cd^{2+} with fulvic acid: A computational chemistry study. *Water Air and Soil Pollution* 183: 467–472.

Seredin VV, Dai SF, Sun YZ, et al. (2013) Coal deposits as promising sources of rare metals for alternative power and energy-efficient technologies. *Applied Geochemistry* 31: 1–11.

Shannon RD (1976) Revised effective ionic radii and systematic studies of interatomic distances in halides and chalcogenides. *Acta Crystallographica Section A* 32: 751–767.

Sun YZ (2015) China geological survey proved the existence of an extra-large coal-associated lithium deposit. *Acta Geologica Sinica (English edition)* 89(1): 311.

Sun YZ, Li YH, Zhao CL, et al. (2010) Concentrations of lithium in Chinese coals. *Energy Exploration & Exploitation* 28(2): 97–104.

Sun YZ, Zhao CL, Li YH, et al. (2012) Li distribution and mode of occurrences in Li-bearing coal seam # 6 from the Guanbanwusu Mine, Inner Mongolia, northern China. *Energy Exploration & Exploitation* 30(1): 109–130.

Sun YZ, Zhao CL, Li YH, et al. (2013a) Further information of the associated Li deposits in the No.6 coal seam at Jungar Coalfield, Inner Mongolia, Northern China. *Acta Geologica Sinica (English Edition)* 87(4): 801–812.

Sun YZ, Zhao CL, Zhang JY, et al. (2013b) Concentrations of valuable elements of the coals from the Pingshuo Mining District, Ningwu Coalfield, Northern China. *Energy, Exploration & Exploitation* 31(5): 727–744.

Sun YZ, Zhao CL, Qin SJ, et al. (2016) Occurrence of some valuable elements in the unique 'high-aluminium coals' from the Jungar Coalfield, China. *Ore Geology Review* 72: 659–668.

Sundararajan M, Rajaraman G and Ghosh SK (2011) Speciation of uranyl ions in fulvic acid and humic acid: A DFT exploration. *Physical Chemistry Chemical Physics* 13: 18038–18046.

Sviatenko LK, Gorb L, Shukla MK, et al. (2016) Adsorption of 2,4,6,8,10,12-hexanitro-2,4,6,8,10,12-hexaazaisowurtzitane (CL-20) on a soil organic matter. A DFT M05 computational study. *Chemosphere* 148: 294–299.

Vasconcelos IF, Haack EA, Maurice PA, et al. (2008) EXAFS analysis of cadmium (II) adsorption to kaolinite. *Chemical Geology* 249(3–4): 237–249.

Wang JX, Wang Q, Shi J, et al. (2015) Distribution and enrichment mode of Li in the No. 11 coal seam from Pingshuo mining district, Shanxi province. *Energy Exploration & Exploitation* 33(2): 203–216.

Zhu X, Chen D and Wu G (2015) Molecular dynamic simulation of asphaltene co-aggregation with humic acid during oil spill. *Chemosphere* 138: 412–421.